

Cosmological constraints from cosmic homogeneity

April 15, 2019

Pierros Ntelis,^{a,1} Adam James Hawken,^a Stephanie Escoffier,^a
Anne Ealet,^b & Andre Tilquin^a

^aAix Marseille University, CNRS/IN2P3, CPPM, Marseille, France

^bInstitut de Physique Nucléaire de Lyon, 69622, Villeurbanne, France

E-mail: pntelis@cppm.in2p3.fr, ealet@cppm.in2p3.fr, escoffier@cppm.in2p3.fr,
hawken@cppm.in2p3.fr, atilquin@cppm.in2p3.fr

Abstract. In this paper, we study the normalised characteristic scale of transition to cosmic homogeneity, \mathcal{R}_H/d_V , as a cosmological probe. We use a compilation of the SDSS galaxy samples, comprising more than 10^6 galaxies in the redshift range $0.17 \leq z \leq 2.2$ within the largest comoving volume to date, $\sim 8h^{-3}\text{Gpc}^3$. We show that these samples can be described by a single bias model as a function of redshift. By combining our measurements with prior Cosmic Microwave Background and Lensing information from the Planck satellite, we constrain the total matter density ratio of the universe $\Omega_m = 0.340 \pm 0.029$ and the Dark Energy density ratio $\Omega_\Lambda = 0.668 \pm 0.023$. Our results are compatible with a flat ΛCDM model. These results show the complementarity of the normalised homogeneity scale with other cosmological probes and open new roads to cosmometry.

Keywords: Cosmology, cosmometry, homogeneity, fractal dimension, observations, large scale structures, gravity, dark energy, ΛCDM

Contents

1	Introduction	2
2	Dataset	3
2.1	Weighting Scheme	3
2.2	Mocks, Bootstraps and Covariance matrices	4
3	Method	5
3.1	Cosmometry with \mathcal{R}_H	5
3.2	Cosmic Bias model for \mathcal{R}_H	6
4	Analysis	7
4.1	Observable Estimation	7
4.2	Bias model selection	8
4.3	MCMC set-up	9
4.4	Results	9
4.5	Study of systematic effects	11
5	Conclusion and Discussion	12
6	Appendix	13

DRAFT

1 Introduction

The best candidate for a Standard Model of Cosmology, is known as the flat Λ CDM model. This gives, to date, the most accurate description of our Universe mainly composed of Cold Dark Matter (CDM) and a cosmological constant Λ , responsible for the accelerating features of our cosmos. The two main assumptions of this model are the validity of General Relativity [1] as an accurate description of gravity and the *Cosmological Principle* [2] that states that the Universe is isotropic and homogeneous on large enough scales. The agreement of this model with current data is excellent, be it from type Ia supernovae [3–6], temperature and polarisation anisotropies in the Cosmic Microwave Background [7, 8], or Large Scale Structure (LSS) [9–14].

Historically, the concept of homogeneity in the large scale structure of the universe can be traced back to Newton [15]. Martínez et al. [16] were the first to measure the homogeneity scale in the distribution of galaxies in the sky, suggesting a value larger than $100 h^{-1}\text{Mpc}$. Since then, several methods have been developed to study the homogeneity scale [17–22]. Most of them found a transition to homogeneity using clustering statistics. For example in Hogg et al. [17], the authors used the fractal dimension obtained from galaxy catalogues from the Sloan Digital Sky Survey (SDSS) to estimate a characteristic homogeneity scale. Evidence for such a scale was found in other surveys as well [23–31]. However, a debate still exists, since some authors claim not to have found such a transition [32–40].

One way to estimate the scale of homogeneity is to use counts-in-spheres. It is expected that, in the specific case of a 3D homogeneous distribution, the number of objects inside a sphere of radius r is $N(< r) \propto r^3$. While in the more general case of a fractal distribution, $N(< r) \propto r^{D_2}$. A characteristic scale of homogeneity can then be defined as the value, \mathcal{R}_H , for which the fractal dimension, D_2 , reaches the nominal homogeneity value, $D_2 = 3$, to some level of precision (in our case 1%) for any redshift. In a recent paper, Ntelis et al. [41] (henceforth N18), we proposed using cosmic homogeneity as a cosmological probe to improve constraints on cosmological parameters. That study was performed using simulations that mimic the Baryon Oscillation Spectroscopy Survey (BOSS) Constant MASS (CMASS) galaxy sample [42]. We studied the more general case of an open- Λ CDM model and we provided evidence that support the flat- Λ CDM hypothesis, in the simulations. In the work presented here, we extend this previous study to real data using galaxy and quasar samples from the public BOSS Data Release (DR) 12 [43] and extended BOSS (eBOSS) DR14 catalogues [44]. We use the fiducial cosmology:

$$p_F = (h, \omega_b, \omega_{\text{cdm}}, n_s, \ln [10^{10} A_s], \Omega_k) = (0.6727, 0.02225, 0.1198, 0.9645, 3.094, 0.0), \quad (1.1)$$

unless stated otherwise, where $h = H_0/[100 \text{ km s}^{-1} \text{ Mpc}^{-1}]$ is the dimensionless Hubble constant, $\omega_b = \Omega_b h^2$, is the reduced baryon density ratio, $\omega_{\text{cdm}} = \Omega_{\text{cdm}} h^2$ is the reduced cold dark matter density ratio, n_s the spectral index, A_s the amplitude of the primordial scalar power spectrum and Ω_k is the curvature density ratio. In this framework, the Dark Energy density ratio is defined via $\Omega_\Lambda = 1 - \Omega_m - \Omega_k$, where $\Omega_m = \Omega_{\text{cdm}} + \Omega_b$ is the total matter density ratio.

The document is structured as follows: In section 2, we describe the galaxy catalogues that we used in our analysis. In section 3, we describe the theoretical framework to put this analysis into context. In section 3.1, we present the main tools that are useful in order to perform cosmometry. In section 3.2, we describe the bias model for the homogeneity scale. In section 4, we describe our analysis. In section 4.1, we describe how to measure the normalised

homogeneity scale in large scale structure surveys. In section 4.2, we describe how we select the bias model for the homogeneity scale. In section 4.3, we set up the Monte Carlo Markov Chain (MCMC) analysis. In section 4.4, we show the results of our analysis. In section 4.5, we present the systematic tests that we performed to ensure the accuracy and precision of our analysis. Finally, in section 5, we discuss our conclusions.

2 Dataset

The Sloan Digital Sky Survey (SDSS) is a suite of surveys using the 2.5-meter Sloan Telescope [45], located at the Apache point Observatory in New Mexico, USA. During SDSS-III [46], the BOSS project [42] collected optical spectra for over a million targets. The spectroscopic galaxy sample of BOSS DR12 [47] is divided into two catalogues: the (Low Redshift) LowZ sample and the CMASS sample.

The sky coverage of the CMASS galaxy sample is $\sim 10,200 \text{ deg}^2$, the LowZ galaxy sample is about $\sim 9,200 \text{ deg}^2$. Objects were selected following the CMASS and LowZ colour cuts described in Reid et al. [48]. For the CMASS sample, we selected objects in the redshift range $0.43 < z < 0.70$, comprising more than 800,000 objects. For the LowZ sample, we use galaxies in the redshift range $0.172 < z < 0.43$, comprising of 400,000 galaxies. Note that, unlike Reid et al. [48], we do not use the galaxies less than $z < 0.172$, since to estimate the error on our observable we need mock catalogues which are not available below that redshift (see section 2.2).

We also use the publicly available Data Release 14 [44] of SDSS from the eBOSS project [42], which contains Luminous Red Galaxies (eLRG) and quasars (QSO). The eLRG sample of the extended survey covers the redshift range $0.6 \leq z \leq 1.0$ over an effective area of about 2000 deg^2 , as selected by Bautista et al. [49]. At higher redshifts, the QSO sample, as selected by Laurent et al. [50] and Zarrouk et al. [51], covers the redshift range $0.8 \leq z \leq 2.2$ with a sky coverage of 2200 deg^2 .

Table 1 summarises our sample, where the number of galaxies is given for the North Galactic Cap (NGC) and the South Galactic Cap (SGC) separately. The eLRG sample is truncated to $0.7 \leq z \leq 0.8$ in order to avoid correlations with CMASS and QSO samples in overlapping regions. The redshift binning was selected such to ensure compatible statistical errors.

2.1 Weighting Scheme

To correct for known clustering systematics, we must apply a particular weight to each galaxy. For LowZ, CMASS and eLRG samples, we follow the weighting scheme [21, 48, 49] where we weight each galaxy according to,

$$\mathcal{W}_{gal} = w_{FKP} * w_{systot} * (w_{cp} + w_{noz} - 1) , \quad (2.1)$$

where w_{FKP} is the common weight accounting for optimisations of the clustering statistics and a luminosity independent clustering bias [52]; $w_{systot} = w_{star} * w_{see}$ is the total angular systematic weight accounting for the seeing effect and the star confusion effect; w_{cp} accounts for the fact that the survey cannot spectroscopically observe two objects that are closer than $62''$ and w_{noz} accounts for redshift failures. For the QSO sample, Zarrouk et al. [51] have shown that in order to account for the efficiency of the instrument at the edges of the focal plane, we need to treat the QSO sample with the weighting scheme:

$$\mathcal{W}_{qso} = w_{FKP} * w_{systot} * w_{cp} * w_{focal} , \quad (2.2)$$

Table 1. The number of galaxies at each redshift bin and the NGC and SGC (North and South Galactic caps) for the four different galaxy types. [See text for details]

	NGC	SGC	Total
LowZ			
0.172 – 0.258	65194	29447	
0.258 – 0.344	97556	41723	
0.344 – 0.430	116690	48333	
0.172 – 0.430	279440	119503	398943
CMASS			
0.430 – 0.484	118757	45601	
0.484 – 0.538	174385	61573	
0.538 – 0.592	150363	55336	
0.592 – 0.700	143566	53531	
0.430 – 0.700	587071	216041	803112
eLRG			
0.700 – 0.800	20801	15489	36290
QSO			
0.800 – 1.150	17911	11560	
1.150 – 1.500	25294	16743	
1.500 – 1.850	25614	17157	
1.850 – 2.200	20422	13976	
0.800 – 2.200	89241	59436	148677

where w_{focal} accounts for the inefficiency of the focal plane of the SDSS telescope. This weighting scheme was shown by the authors to give better estimates of clustering statistics and we expect the same for our statistic.

2.2 Mocks, Bootstraps and Covariance matrices

To estimate the errors and covariance matrices in this analysis we used mock catalogues and the bootstrap internal sampling method. We used the Quick Particle Mesh (QPM) mock galaxy catalogues produced by White et al. [53]. The method is based on using quick, low-resolution particle mesh simulations that accurately reproduce the large scale dark matter density field. Particles are then sampled from the density field based on their local density such that they have N-point statistics nearly equivalent to the halos resolved in high-resolution simulations. These simulations are used to create a set of mock halos that can be populated using halo occupation methods to create galaxy mocks. Then the survey geometry is imprinted on those catalogues to produce the mock catalogues that we use in this study. The cosmology used to obtain these catalogues is:

$$p_{qpm} = (h, \omega_b, \omega_{cdm}, n_s, \ln [10^{10} A_s], \Omega_k) = (0.7, 0.0225, 0.11172, 0.95, 3.077, 0.0). \quad (2.3)$$

The SDSS collaboration has available the QPM mock catalogues for the LowZ and CMASS samples. We used 100 of them to compute the covariance matrix of the fractal dimension \mathcal{D}_2 , see section 3.

Mock catalogues were not available at the time for the eLRG and QSO samples, so we used a bootstrap internal sampling method. The bootstrap method consists of subsampling each galaxy catalogue with replacement. Then we compute \mathcal{D}_2 for each sub-sampled catalogue to produce the covariance matrix. For either method the covariance matrix is given by:

$$C_{ij} = \frac{1}{N_r - 1} \sum_{n=1}^{N_r} \left(\mathcal{D}_2^{(n)}(r_i) - \bar{\mathcal{D}}_2(r_i) \right) \left(\mathcal{D}_2^{(n)}(r_j) - \bar{\mathcal{D}}_2(r_j) \right), \quad (2.4)$$

where N_r is the number of realisations. For our fitting method, we corrected our precision matrix following Taylor et al. [54], using $\psi_{ij} = \frac{N_r - N_d - 2}{N_r - 1} C_{ij}^{-1}$, where N_d is the number of data bins.

3 Method

In this paper, we are interested in the theoretical prediction of a characteristic scale of homogeneity of the universe, \mathcal{R}_H (henceforth homogeneity scale), for a given theoretical model, in our case the open- Λ CDM model. This homogeneity scale, following N18 and references therein, can be defined as the scale at which the fractal dimension, D_2 , takes the value corresponding to a three dimensional homogeneous distribution to within 1% precision, formally written as:

$$\mathcal{D}_2(\mathcal{R}_H) = 2.97, \quad (3.1)$$

where the fractal correlation dimension is given by,

$$\mathcal{D}_2(r) = \frac{d \ln}{d \ln r} \left[1 + \frac{3}{r^3} \int_0^r \xi(s) s^2 ds \right] + 3, \quad (3.2)$$

where ξ is the two-point correlation function. The two point correlation function is related to the Power Spectrum, $P(k)$, through the Fourier Transform,

$$\xi(r) = \frac{1}{2\pi^2} \int dk k^2 \frac{\sin(kr)}{kr} P(k). \quad (3.3)$$

In order to retrieve all these related quantities, we use the CLASS code[55] to solve the perturbed Einstein-Boltzman equation to obtain $P(k)$ for a given cosmology. We have made our codes for the computation of the homogeneity scale and related quantities publicly available¹.

3.1 Cosmometry with \mathcal{R}_H

From the observational point of view, we need to infer distances from $(z, R.A., Dec)$ positions of galaxies. Therefore, we transform them into comoving coordinates in the following way. It is convenient to introduce the following quantities. The *comoving distance*:

$$d_C(z) = d_H \int_0^z dz' E^{-1}(z'), \quad (3.4)$$

where $d_H = c/H_0$, H_0 is the Hubble expansion rate today, c is the speed of light and

$$E(z) \equiv \frac{H(z)}{H_0} = \sqrt{(\Omega_{\text{cdm}} + \Omega_b)(1+z)^3 + \Omega_\Lambda + \Omega_k(1+z)^2},$$

¹<https://github.com/lontelis/cosmopit>

is the usual normalised Hubble expansion rate as a function of redshift depending on the standard cosmological components of the universe, $\Omega_X = \{\Omega_{cdm}, \Omega_b, \Omega_\Lambda, \Omega_k\}$. The cube of the *volume distance* (or comoving volume element),

$$d_V^3(z) = \frac{cz}{H(z)} d_M^2(z), \quad (3.5)$$

where d_M is the *motion distance* (or transverse comoving distance).

Having these tools to hand, we use the Landy and Szalay [56] estimator to extract the two-point correlation function from the positions of galaxies in the catalogue. From this, using Eq. 3.2 and Eq. 3.1, we extract the fractal dimension and the homogeneity scale. Now using Eq. 3.5, we normalise the homogeneity scale, according to Rich [57], which defines our observable:

$$O(z) = \frac{\mathcal{R}_H(z)}{d_V(z)} \quad (3.6)$$

for different redshift slices and for a given fiducial cosmology. This normalisation ensures that the observable is independent of the h parameter.

Keep in mind that our observable is biased with respect to the total matter of the universe, therefore we take that into account as we explain in section 3.2. Additionally, the likelihood may be biased towards the fiducial cosmology and we study this effect in section 4.5.

3.2 Cosmic Bias model for \mathcal{R}_H

The homogeneity scale for a given tracer of matter, such as the galaxy distribution, \mathcal{R}_H^G , is related to the homogeneity scale of the matter distribution, \mathcal{R}_H^m ,

$$\mathcal{R}_H^G(z) = b_{\mathcal{R}_H}(z) \mathcal{R}_H^m(z), \quad (3.7)$$

where $b_{\mathcal{R}_H}(z)$ is the bias model as a function of redshift. The different galaxy samples that we are using may potentially have a different bias. This means that the number of parameters of our model will be large and potentially we will not be able to constrain cosmological parameters with few data bins. In order to have a small number of parameters in the bias model, we investigate the possibility of modelling the bias with one single model for all galaxy samples. For that reason we investigate two different bias models. The first one is:

$$b_{1, \mathcal{R}_H}(z) = b_0 \sqrt{1+z} \quad (3.8)$$

following Amendola et al. [58], Montanari and Durrer [59].

The second one is a piecewise linear bias model as a function of redshift. For lower redshifts $z < z_*$, we use the linear bias:

$$b_{\mathcal{R}_H}^{z < z_*}(z; b_0) = b_0 \sqrt{1+z} \quad (3.9)$$

while for the higher redshift QSO sample, the cosmic bias, according to Laurent et al. [60], is:

$$b_{\mathcal{R}_H}^{z > z_*}(z; b_1, b_2) = b_1 * (1+z)^2 + b_2. \quad (3.10)$$

We make the assumption that there is a continuity between the lower redshifts and higher redshifts at $z \sim z_*$ and therefore we impose the following continuity conditions between the two redshift regions:

$$b^{z < z_*}(z = z_*) = b^{z > z_*}(z = z_*) \quad (3.11)$$

$$\frac{\partial b^{z < z_*}}{\partial z} \Big|_{z=z_*} = \frac{\partial b^{z > z_*}}{\partial z} \Big|_{z=z_*} \quad (3.12)$$

After some algebra we find that:

$$b_1 = \frac{1}{4} \frac{1}{(1+z_\star)^{3/2}} b_0 \quad (3.13)$$

$$b_2 = \frac{3}{4} \sqrt{1+z_\star} b_0 \quad (3.14)$$

Now, Eq. 3.10 can be re-written, as a function of b_0 and z_\star as:

$$b_{\mathcal{R}_H}^{z > z_\star}(z; b_0) = b_0 \left[\frac{1}{4} \frac{1}{(1+z_\star)^{3/2}} (1+z)^2 + \frac{3}{4} \sqrt{1+z_\star} \right]. \quad (3.15)$$

Therefore, the cosmic bias model for the homogeneity scale at redshifts $0.0 < z < 2.2$ can be written as :

$$b_{2, \mathcal{R}_H}(z; b_0, z_\star) = b_0 \left\{ \begin{array}{l} \sqrt{1+z} \\ \left[\frac{1}{4} \frac{1}{(1+z_\star)^{3/2}} (1+z)^2 + \frac{3}{4} \sqrt{1+z_\star} \right] \end{array} \right. , \text{ for } z < z_\star \left. \vphantom{b_{2, \mathcal{R}_H}} \right\}. \quad (3.16)$$

We choose $z_\star = 0.8$ which is the redshift where the QSO sample starts. In section 4.2, we test both of the above bias models against the data.

4 Analysis

In this section, we describe our analysis given the method described in section 3. We briefly describe the estimation of the normalised homogeneity scale as obtained from the different galaxy catalogues. Then we describe the method that we used in order to choose the best bias model for the homogeneity scale. Then we present the Monte Carlo Markov Chain (MCMC) analysis that we performed in order to constrain cosmology. We also present the test against the fiducial cosmology.

4.1 Observable Estimation

For each of the galaxy samples described in section 2, the fractal dimension, $\mathcal{D}_2(r)$, as defined in Eq. 3.2, is computed over the range $r = [50, 200]h^{-1}\text{Mpc}$, at each redshift bin. We use the 100 QPM mocks (or 100 bootstraps, see section 2.2) for the different redshift bins to construct the covariance matrix of \mathcal{D}_2 . The function, \mathcal{D}_2 , is then fitted by a spline. The homogeneity scale of the galaxy samples, \mathcal{R}_H^G is then the scale at which this spline crosses $\mathcal{D}_2 = 2.97$. extracted using the definition given in Eq. 3.1.

Table 2 shows the estimated homogeneity scale, \mathcal{R}_H^G , the theoretical homogeneity scale for the total matter, \mathcal{R}_H^m , and the volume distance, d_V , for the different galaxy samples in the different redshift bins.

Since we make estimates from the galaxy samples, our observable is given by:

$$O(z) = \frac{\mathcal{R}_H^G(z)}{d_V(z)}, \quad (4.1)$$

while the theoretical expectation is given by:

$$M(z) = \frac{\mathcal{R}_H^m(z)}{d_V(z)} b_{i, \mathcal{R}_H}(z) \quad (4.2)$$

where $i = 1, 2$ for the two different bias models that we study (see section 3.2).

Table 2. Mean and standard deviation of the homogeneity scale, \mathcal{R}_H , as a function of redshift, z , for the different galaxy samples as explained in section 4.1. The second to last column is the expected homogeneity scale for the total matter of the universe, \mathcal{R}_H^m , while the last column is the fiducial volume distance, see d_V section 4.1.

	\mathcal{R}_H^G [$h^{-1}\text{Mpc}$]				\mathcal{R}_H^m [$h^{-1}\text{Mpc}$]	d_V [$h^{-1}\text{Mpc}$]
	LowZ	CMASS	eLRG	QSO		
0.172 – 0.258	109.54 ± 6.81	-	-	-	73.87	600
0.258 – 0.344	132.51 ± 9.87	-	-	-	70.87	813
0.344 – 0.430	127.87 ± 5.95	-	-	-	68.0	1012
0.430 – 0.484	-	120.32 ± 5.33	-	-	65.80	1163
0.484 – 0.538	-	116.16 ± 3.98	-	-	64.16	1274
0.538 – 0.592	-	112.24 ± 3.97	-	-	62.55	1379
0.592 – 0.700	-	115.50 ± 3.00	-	-	60.25	1529
0.700 – 0.800	-	-	117.60 ± 5.50	-	57.45	1704
0.800 – 1.150	-	-	-	95.08 ± 6.72	51.96	2033
1.150 – 1.500	-	-	-	98.15 ± 6.87	44.78	2430
1.500 – 1.850	-	-	-	97.65 ± 6.50	38.96	2726
1.850 – 2.200	-	-	-	101.45 ± 7.67	34.17	2952

4.2 Bias model selection

In order to select one bias model for all redshifts, we kept the fiducial cosmology fixed and we fitted the parameters of the bias model. We performed the fit for each sample separately, at low redshift with Eq. 3.9. We fitted the b_0 parameter at each sample, LowZ, CMASS, eLRG. While for high redshifts we fitted the bias model Eq. 3.10 with two free parameters, b_1, b_2 .

Figure 1 shows the normalised homogeneity scale as measured in our four galaxy samples, LowZ (blue), CMASS (purple), eLRG (yellow) and QSO (green). The coloured bands represent the 2σ uncertainty on the best fitting bias parameters for each sample, as described above.

Table 3. Measurement of the cosmological parameters for the two different bias models, as described in section 4.2, considering the combination, $b_{i,\mathcal{R}_H}-\mathcal{R}_H/d_V+\text{CMB}+\text{Lensing}$.

Bias model	b_0	Ω_m	Ω_Λ	$\chi^2 \pm \sqrt{2 \cdot ndf}$, $ndf = 9$
b_{1,\mathcal{R}_H}	1.747 ± 0.136	0.340 ± 0.029	0.668 ± 0.023	16.476 ± 4.243
b_{2,\mathcal{R}_H}	1.886 ± 0.184	0.311 ± 0.030	0.690 ± 0.024	17.569 ± 4.243

The different bias parameters are highly compatible with one another. For example, the best fitting bias model for the QSO sample and the best fitting bias model for the eLRG sample, are compatible to the level of $\chi^2 = 1.4\sigma_T$. This justifies the fact that we can use the same bias model at all redshifts. In order to select the best bias model between the two candidates, Eq. 3.9 and Eq. 3.16, we performed a test. We fitted the two models to the data, and we investigated the χ^2 . In table 3, we show that the first model performs better since it has a lower χ^2 . We repeated this test using the p_{qpm} fiducial cosmology on the data and we obtained similar results. Henceforth, all the results we present have been found using the first bias model.

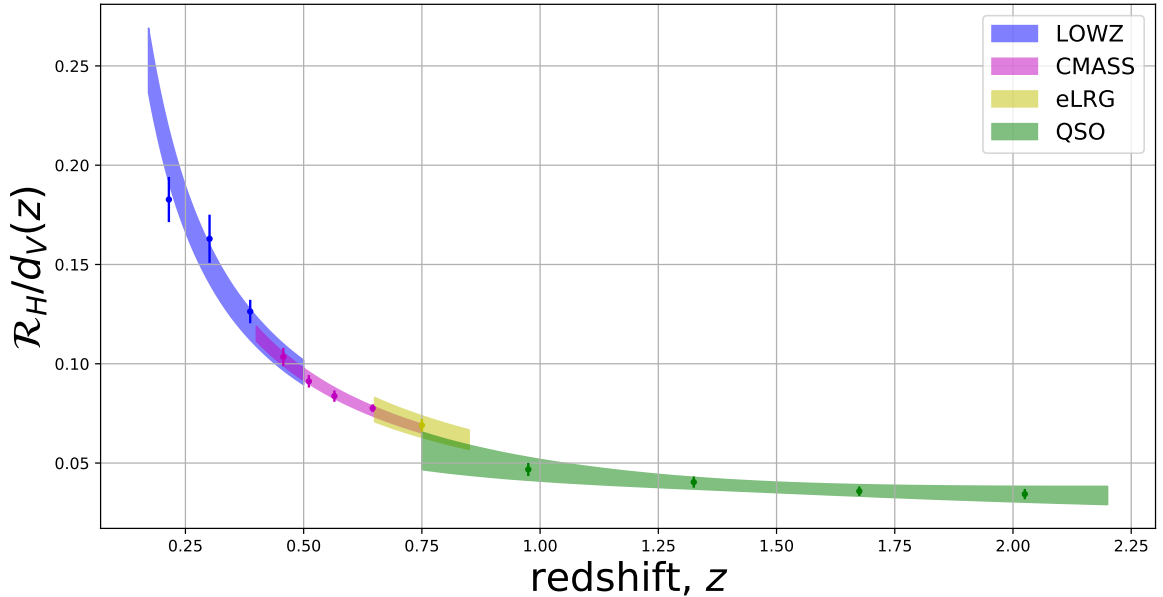


Figure 1. The normalised homogeneity scale as a function of redshift, for the different galaxy samples, colorcoded. The shade areas show the 2σ deviation of the fiducial model fitted to the data for the different parametrisation of the bias for the different galaxies sample. [see section 4.2]

4.3 MCMC set-up

We used an MCMC² to sample the posterior probability distribution of our cosmological parameter space $p = (b_0, \Omega_m, \Omega_\Lambda)$, to determine the cosmological constraints provided by the normalised homogeneity scale. The likelihood for a given set of cosmological parameters, θ , is expressed as $\mathcal{L}(p) \propto \exp[-\chi^2(p)/2]$, where χ^2 is:

$$\chi^2(\theta) = \Delta(p)\mathbf{C}^{-1}\Delta^T(p), \quad (4.3)$$

where \mathbf{C} is the covariance matrix, and $\Delta(p) = \mathbf{O} - \mathbf{M}(p)$; \mathbf{M} is the theoretical prediction; \mathbf{O} is our observable, given by Eq. 4.1. We looked for covariance between the redshift bins and found it to be negligible. Therefore, we only used the diagonal of the covariance matrix.

In order to accelerate our MCMC, we computed $\mathcal{R}_H^M(z)$ on a grid of 20^3 for the $z, \Omega_m, \Omega_\Lambda$ parameters, and we used a 3D interpolation method to obtain the theoretical prediction of the homogeneity scale. We ran our MCMC with flat priors $0.0 \leq z \leq 2.2$, $0.2 \leq \Omega_m \leq 0.9$ and $0.4 \leq \Omega_\Lambda \leq 0.9$.

In addition to our observable, we also used prior information on the $(\Omega_m, \Omega_\Lambda)$ plane as obtained by Planck 2018 [7] from the CMB and the CMB+Lensing measurements.

4.4 Results

In Fig. 2, we present the normalised homogeneity scale for the galaxy distribution of the universe as a function of redshift. The quantity, \mathcal{R}_H/d_V , is plotted for the four galaxy samples that we study, i.e. the LowZ sample (blue), the CMASS sample (magenta), eLRG

²We used the publicly available code, pymc <https://pymc-devs.github.io/pymc/>.

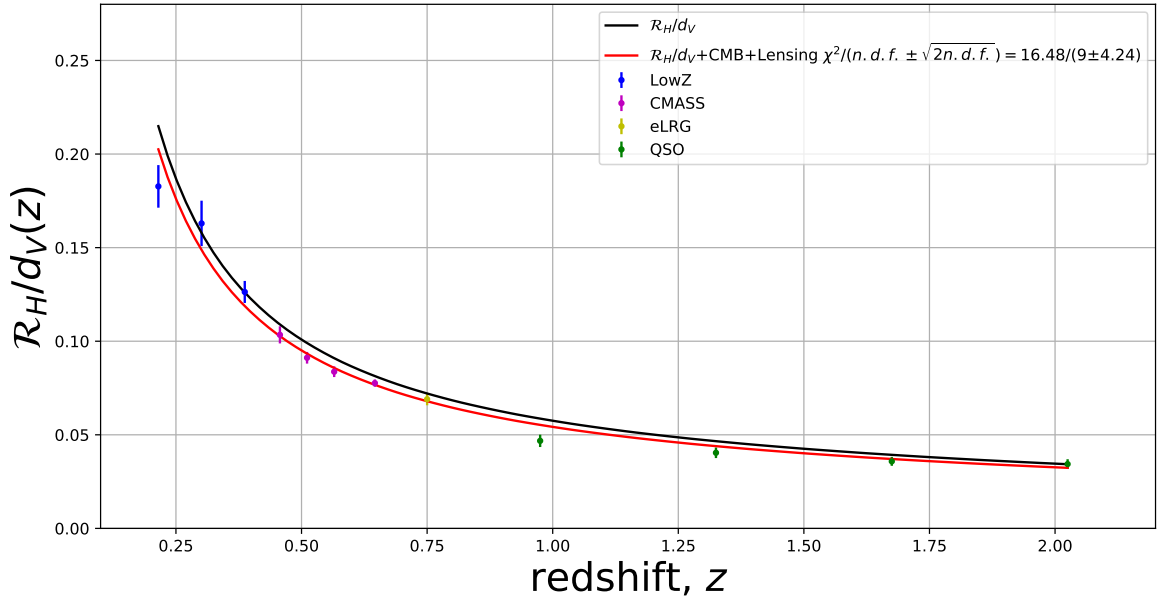


Figure 2. Redshift evolution of the normalised homogeneity scale for the four data galaxy samples, LowZ(blue), CMASS (purple), eLRG (yellow) and QSO (green). The black line is the model that best fits the data alone. [see section 4.4].

sample (yellow) and the QSO sample (green). Figure 2 also shows the two best fitting models, one using only the galaxy data, the other one obtained in combination with CMB+Lensing.

In Fig. 3, we present the result of our MCMC analysis for the open Λ CDM model. We show the marginalised contours of the 6 different combinations of the $(b_0, \Omega_m, \Omega_\Lambda)$ planes for the \mathcal{R}_H/d_V alone (black), CMB+Lensing (blue), and the combination of \mathcal{R}_H/d_V +CMB+Lensing (red). The green star denotes the values of the fiducial cosmology. The results for the probe combinations that we studied in this work, are shown in table 4.

Table 4. Mean and standard deviation of the measured cosmological parameters $(\Omega_m, \Omega_\Lambda)$, using different combination of data. [See section 4.4]

Observable Combinations	Ω_m	Ω_Λ
CMB	0.473 ± 0.089	0.571 ± 0.070
CMB + Lensing	0.352 ± 0.036	0.658 ± 0.029
\mathcal{R}_H/d_V	0.338 ± 0.059	0.653 ± 0.133
$\mathcal{R}_H/d_V + \text{CMB}$	0.369 ± 0.062	0.651 ± 0.073
$\mathcal{R}_H/d_V + \text{CMB} + \text{Lensing}$	0.340 ± 0.029	0.668 ± 0.023

We find that \mathcal{R}_H/d_V alone can constrain the measurement of Ω_m . The addition of information from \mathcal{R}_H/d_V improves constraints relative to the CMB alone with 33% reduction of the uncertainty for Ω_m and 26% for Ω_Λ . While when we add the normalised homogeneity scale to the CMB+Lensing we have an improvement of a 20% reduction of the uncertainty for Ω_m and 21% for Ω_Λ . These results show that the combination of the homogeneity scale

with the CMB provides results comparable to CMB+Lensing.

These results demonstrate that \mathcal{R}_H/d_V can be used as a probe to constrain cosmological parameters. In particular, it can be used to improve the cosmological measurements in the $(\Omega_m, \Omega_\Lambda)$ plane³.

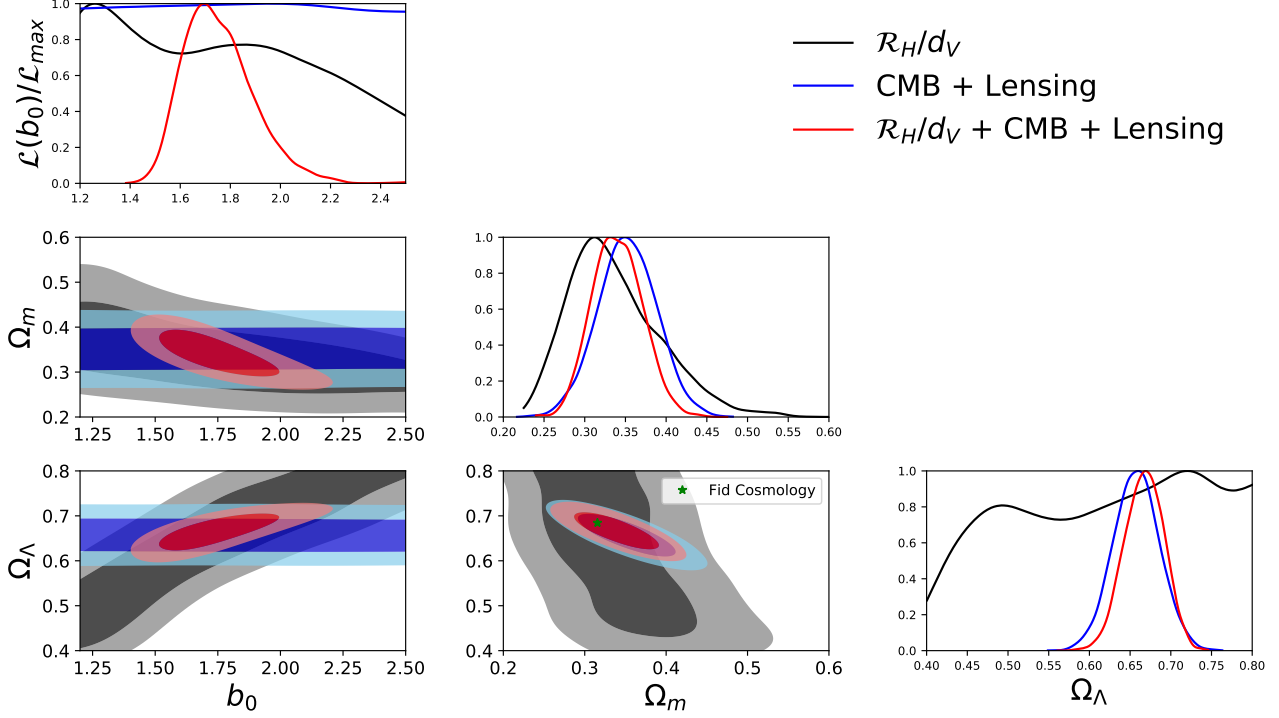


Figure 3. Contours of 68% (dark) and 95% (light) C.L. of $(b_0, \Omega_m, \Omega_\Lambda)$ planes using actual data, \mathcal{R}_H/d_V (black), CMB+Lensing (blue) and \mathcal{R}_H/d_V +CMB+Lensing (red). The green star denotes the values of our fiducial cosmology. The diagonal panels show the normalised likelihood and the mean and the standard deviation of each parameter colour-coded for each probe. [See text for section 4.4]

Table 5. Measurements of the model parameters using bias model 1, Eq. 3.16. [See section 4.5]

$b_{1, \mathcal{R}_H}(z)$	b_0	Ω_m	Ω_Λ	$\chi^2 \pm \sqrt{2 \cdot ndf}, ndf = 9$
p_F - \mathcal{R}_H/d_V +CMB	1.693 ± 0.218	0.369 ± 0.060	0.651 ± 0.052	23.708 ± 4.243
p_{qpm} - \mathcal{R}_H/d_V +CMB	1.690 ± 0.218	0.366 ± 0.059	0.653 ± 0.051	22.839 ± 4.243
p_F - \mathcal{R}_H/d_V +CMB+Lensing	1.747 ± 0.136	0.340 ± 0.029	0.668 ± 0.023	16.476 ± 4.243
p_{qpm} - \mathcal{R}_H/d_V +CMB+Lensing	1.740 ± 0.137	0.339 ± 0.030	0.668 ± 0.023	15.945 ± 4.243

4.5 Study of systematic effects

In order to quantify any bias coming from the values of the fiducial cosmology, we performed a dedicated study. We repeated the measurement on the data using the cosmology from

³Our analysis is available under GNU licence <https://github.com/lontelis/CoHo2>.

the mock catalogues as the fiducial cosmology. The two different cosmologies are defined by Eq. 1.1 (denoted by p_F) and Eq. 2.3 (denoted by p_{ppm}). These cosmologies differ from each other by 15% for Ω_m and by 6% for Ω_Λ . We present the results in table 5. The systematic bias obtained by the different fiducial cosmologies is not significant with respect to the statistical error. Ideally, this study should be performed on mock catalogues, but there are not publicly available mocks at all redshift bins.

5 Conclusion and Discussion

In this work, we have demonstrated that the normalised characteristic scale of transition to cosmic homogeneity, \mathcal{R}_H/d_V , can be used as a cosmological probe with large scale structure surveys. For this, we have used four publicly available galaxy samples, LowZ, CMASS, eLRG and QSO of the Sloan Digital Sky Survey. We have also used an empirical approach in order to extract a redshift dependent bias model for the normalised homogeneity scale at all redshifts from the different galaxy samples.

In order to quantify the additional cosmological information contained in the normalised homogeneity scale, we have performed an MCMC analysis and we have explored the open Λ CDM model. By combining our measurements with CMB+Lensing prior information, we found $\Omega_m = 0.340 \pm 0.029$ and $\Omega_\Lambda = 0.668 \pm 0.023$, consistent with a flat Λ CDM cosmological model at the 1σ level. The inclusion of \mathcal{R}_H/d_V improves CMB+Lensing constraints alone by a reduction on the uncertainty of the order of 20% for Ω_m and 21% for Ω_Λ . There is, therefore, a clear gain when it is combined with CMB+Lensing information.

The normalised homogeneity scale shows evidence for a flat- Λ CDM cosmology. This is in agreement with current literature on the combination of galaxy clustering and other probes [7]. In particular, we find $\Omega_k = -0.0072 \pm 0.0079$ which is comparable to the Planck value, $\Omega_k^{\text{CMB+Lensing+BAO}} = 0.0007 \pm 0.0019$. The BAO analysis performed in Aghanim et al. [7], takes into account two dimensional information from galaxy clustering, r_\perp, r_\parallel . In contrast, in this work, we have not taken that into account, which might result in our lower constraining power. Therefore, further studies are required with more sophisticated analysis to combine this measurement with other probes.

In this work, we measured the homogeneity scale on the QSO sample independently from Laurent et al. [20], Gonçalves et al. [22]. We acquired results that are compatible and more precise. We have more precise results than Gonçalves et al. [22], since they used narrower redshift bins than us. Laurent et al. [20] have used an outdated QSO catalogue from BOSS, while we are using the eBOSS QSO catalogue which is both deeper and denser. Therefore, we get more precise measurements.

Nesseris and Trashorras [61] have argued that the homogeneity scale cannot be considered as a standard ruler and that it cannot constrain cosmological parameters since it does not have a one-to-one dependence on Ω_m . We agree with the first statement. Since \mathcal{R}_H evolves with time (and therefore redshift) it cannot be considered to be a standard ruler. However, we disagree with their second conclusion. In this paper, we have shown that the normalised homogeneity scale, \mathcal{R}_H/d_V , without the addition of other probes, can be used to place a constraint on Ω_m . In addition we have shown that in combination with CMB+Lensing, the normalised homogeneity scale also improves the constraint on Ω_m and Ω_Λ .

In conclusion, we have revealed the complementarity of the homogeneity scale with respect to other cosmological probes.

Finally, we stress that this analysis can be performed and improved upon in the light of more observational data from current and future survey such as SDSS-IV[62], DESI[63], Euclid[64] and LSST[65]. Furthermore, analogous methods could be applied to data from SKA[66]. A similar analysis can also be applied by measuring the normalised homogeneity in the temperature fluctuations of CMB as observed by Planck [7]. Potentially, one could investigate additional observational systematic effects on our probe [67], but as shown in [68] the known systematics (modelled by the weights), do not affect the measurement of the homogeneity scale at the 1σ level. One can also extend this analysis to test Modified Gravity models or Effective Field Theory models[64]. We leave these analyses for future work.

ACKNOWLEDGEMENTS

We would like to thank Christian Marinoni, Julien Bel, Jean-Marc Le Goff, James Rich, Jean-Christophe Hamilton, Adam Morris and Francis Bernardeau for useful suggestions and discussions.

PN is funded by 'Centre National d'étude spatiale' (CNES), for the Euclid project.

AJH acknowledges the financial support of the OCEVU LABEX (Grant No. ANR-11-LABX-0060) and the A*MIDEX project (Grant No. ANR-11-IDEX- 0001- 02) funded by the Investissements d'Avenir french government program managed by the ANR. This work also acknowledges support from the ANR eBOSS project (under reference ANR-16-CE31-0021) of the French National Research Agency.

This research used resources of the IN2P3/CNRS and the Dark Energy computing Center funded by the OCEVU Labex (ANR-11-LABX-0060).

The French Participation Group of SDSS was supported by the French National Research Agency under contracts ANR-08-BLAN-0222, ANR-12-BS05-0015-01 and ANR-16-CE31-0021.

Funding for SDSS-III has been provided by the Alfred P. Sloan Foundation, the Participating Institutions, the National Science Foundation, and the U.S. Department of Energy Office of Science. The SDSS-III web site is <http://www.sdss3.org/>.

SDSS-III is managed by the Astrophysical Research Consortium for the Participating Institutions of the SDSS-III Collaboration including the University of Arizona, the Brazilian Participation Group, Brookhaven National Laboratory, Carnegie Mellon University, University of Florida, the French Participation Group, the German Participation Group, Harvard University, the Instituto de Astrofísica de Canarias, the Michigan State/Notre Dame/JINA Participation Group, Johns Hopkins University, Lawrence Berkeley National Laboratory, Max Planck Institute for Astrophysics, Max Planck Institute for Extraterrestrial Physics, New Mexico State University, New York University, Ohio State University, Pennsylvania State University, University of Portsmouth, Princeton University, the Spanish Participation Group, University of Tokyo, University of Utah, Vanderbilt University, University of Virginia, University of Washington, and Yale University.

6 Appendix

In table 6, we summarise the fiducial cosmology values and the measured values used in this study

Table 6. Reference table for the $(\Omega_m, \Omega_\Lambda)$ -plane. The first two lines show the fiducial cosmology used in this work, the last two lines show the cosmology measurements as obtained by Planck 2018 [7].

	b_0	Ω_m	Ω_Λ
Data - Fiducial (p_F)	–	0.316	0.684
Mock - QPM Fiducial (p_{qpm})	–	0.274	0.726
CMB (Planck 2018)	–	0.473 ± 0.089	0.571 ± 0.072
CMB+Lensing(Planck 2018)	–	0.352 ± 0.036	0.658 ± 0.029

References

- [1] Albert Einstein. Kosmologische und Relativitätstheorie. *SPA der Wissenschaften*, 142, 1917.
- [2] George FR Ellis. Cosmology and verifiability. *Quarterly Journal of the Royal Astronomical Society*, 16:245–264, 1975.
- [3] Saul Perlmutter, G Aldering, G Goldhaber, et al. Measurements of Ω and Λ from 42 high-redshift supernovae. *The Astrophysical Journal*, 517(2):565, 1999.
- [4] Adam G Riess, Alexei V Filippenko, Peter Challis, et al. Observational evidence from supernovae for an accelerating universe and a cosmological constant. *The Astronomical Journal*, 116(3):1009, 1998.
- [5] M. Betoule, R. Kessler, J. Guy, J. Mosher, and C. J. Improved cosmological constraints from a joint analysis of the SDSS-II and SNLS supernova samples. 568:A22, August 2014. doi: 10.1051/0004-6361/201423413.
- [6] DES Collaboration, T. M. C. Abbott, S. Allam, et al. First Cosmology Results using Type Ia Supernovae from the Dark Energy Survey: Constraints on Cosmological Parameters. *ArXiv e-prints*, November 2018.
- [7] N Aghanim, Y Akrami, M Ashdown, et al. Planck 2018 results. VI. Cosmological parameters. *arXiv preprint arXiv:1807.06209*, 2018.
- [8] DJ Fixsen, ES Cheng, JM Gales, et al. The Cosmic Microwave Background Spectrum from the Full COBE FIRAS Data Set. *The Astrophysical Journal*, 473(2):576, 1996.
- [9] Daniel J Eisenstein, Idit Zehavi, David W Hogg, et al. Detection of the baryon acoustic peak in the large-scale correlation function of SDSS luminous red galaxies. *The Astrophysical Journal*, 633(2):560, 2005.
- [10] WJ Percival et al. Parameter constraints for flat cosmologies from cmb and 2dfgrs power spectra, 2002. *Mon. Not. R. Astron. Soc.*, 337:1068.
- [11] David Parkinson, Signe Riemer-Sørensen, Chris Blake, et al. The wigglez dark energy survey: final data release and cosmological results. *Physical Review D*, 86(10):103518, 2012.
- [12] Catherine Heymans, Emma Grocutt, Alan Heavens, Martin Kilbinger, et al. CFHTLenS tomographic weak lensing cosmological parameter constraints: Mitigating the impact of intrinsic galaxy alignments. *Monthly Notices of the Royal Astronomical Society*, 432(3): 2433–2453, 2013.
- [13] Éric Aubourg, Stephen Bailey, Florian Beutler, et al. Cosmological implications of baryon acoustic oscillation measurements. *Physical Review D*, 92(12):123516, 2015.
- [14] S. Alam, M. Ata, S. Bailey, et al. The clustering of galaxies in the completed SDSS-III Baryon Oscillation Spectroscopic Survey: cosmological analysis of the DR12 galaxy sample. *Monthly Notices of the RAS*, 470:2617–2652, September 2017. doi: 10.1093/mnras/stx721.

- [15] Isaac Newton. *Philosophiæ naturalis principia mathematica, vol. 1 - 4*. 1760.
- [16] Vicent J Martínez, Maria-Jesus Pons-Borderia, Rana A Moyeed, and Matthew J Graham. Searching for the scale of homogeneity. *Monthly Notices of the Royal Astronomical Society*, 298(4):1212–1222, 1998.
- [17] D. W. Hogg, D. J. Eisenstein, M. R. Blanton, et al. Cosmic homogeneity demonstrated with luminous red galaxies. *The Astrophysical Journal*, 624(1):54, 2005.
- [18] Jaswant Yadav, Somnath Bharadwaj, Biswajit Pandey, and TR Seshadri. Testing homogeneity on large scales in the Sloan Digital Sky Survey data release one. *Monthly Notices of the Royal Astronomical Society*, 364(2):601–606, 2005.
- [19] Prakash Sarkar, Jaswant Yadav, Biswajit Pandey, and Somnath Bharadwaj. The scale of homogeneity of the galaxy distribution in SDSS DR6. *Monthly Notices of the Royal Astronomical Society: Letters*, 399(1):L128–L131, 2009.
- [20] P. Laurent, J.-M. Le Goff, E. Burtin, et al. "A $14 \text{ h}^{-3} \text{ Gpc}^3$ study of cosmic homogeneity using BOSS DR12 quasar sample". 11:060, November 2016. doi: 10.1088/1475-7516/2016/11/060.
- [21] Pierros Ntelis, Jean-Christophe Hamilton, Nicolas Guillermo Busca, et al. Exploring cosmic homogeneity with the BOSS DR12 galaxy sample. *arXiv preprint arXiv:1702.02159*, 2017.
- [22] R. S. Gonçalves, G. C. Carvalho, C. A. P. Bengaly, J. C. Carvalho, and J. S. Alcaniz. Measuring the scale of cosmic homogeneity with SDSS-IV DR14 quasars. *ArXiv e-prints*, art. arXiv:1809.11125, September 2018.
- [23] Luca Amendola and Emilia Palladino. The scale of homogeneity in the Las Campanas Redshift Survey. *The Astrophysical Journal Letters*, 514(1):L1, 1999.
- [24] R Scaramella, L Guzzo, G Zamorani, et al. The ESO Slice Project [ESP] galaxy redshift survey: V. Evidence for a $D=3$ sample dimensionality. 1998.
- [25] Jun Pan and Peter Coles. Large-scale cosmic homogeneity from a multifractal analysis of the PSCz catalogue. *Monthly Notices of the Royal Astronomical Society*, 318(4):L51–L54, 2000.
- [26] T Kurokawa, M Morikawa, and H Mouri. Scaling analysis of galaxy distribution in the Las Campanas Redshift Survey data. *Astronomy & Astrophysics*, 370(2):358–364, 2001.
- [27] C. Marinoni, J. Bel, and A. Buzzi. The scale of cosmic isotropy. *Journal of Cosmology and Astro-Particle Physics*, 2012:036, October 2012. doi: 10.1088/1475-7516/2012/10/036.
- [28] M. I. Scrimgeour, T. Davis, C. Blake, J. B. James, et al. The WiggleZ Dark Energy Survey: the transition to large-scale cosmic homogeneity. *Monthly Notices of the Royal Astronomical Society*, 425(1):116–134, 2012.
- [29] Felipe Avila, Camila P Novaes, Armando Bernui, and E de Carvalho. The scale of homogeneity in the local Universe with the ALFALFA catalogue. *arXiv preprint arXiv:1806.04541*, 2018.

- [30] Stephen Appleby and Arman Shafieloo. Testing isotropy in the local Universe. *Journal of Cosmology and Astroparticle Physics*, 2014(10):070, 2014.
- [31] James. P. Zibin and Adam Moss. Nowhere to hide: closing in on cosmological homogeneity. *arXiv e-prints*, art. arXiv:1409.3831, September 2014.
- [32] F Sylos Labini, M Montuori, and L Pietronero. Comment on the paper by L. Guzzo " Is the Universe homogeneous?". 1998.
- [33] Paul H Coleman and Luciano Pietronero. The fractal structure of the universe. *Physics Reports*, 213(6):311–389, 1992.
- [34] L. Pietronero, M. Montuori, and F. Sylos Labini. On the Fractal Structure of the Visible Universe. In Neil Turok, editor, *Critical Dialogues in Cosmology*, page 24, January 1997.
- [35] F Sylos Labini, Marco Montuori, and Luciano Pietronero. Scale-invariance of galaxy clustering. *Physics Reports*, 293(2):61–226, 1998.
- [36] F Sylos Labini. Breaking the self-averaging properties of spatial galaxy fluctuations in the sloan digital sky survey–data release six. *Astronomy & Astrophysics*, 508(1):17–43, 2009.
- [37] F Sylos Labini. Very large-scale correlations in the galaxy distribution. *EPL (Europhysics Letters)*, 96(5):59001, 2011.
- [38] Michael Joyce, Marco Montuori, and F Sylos Labini. Fractal correlations in the cfa2-south redshift survey. *The Astrophysical Journal Letters*, 514(1):L5, 1999.
- [39] Chan-Gyung Park, Hwasu Hyun, Hyerim Noh, and Jai-chan Hwang. The cosmological principle is not in the sky. *Monthly Notices of the Royal Astronomical Society*, 469(2):1924–1931, 2017.
- [40] J. Gaite. The projected mass distribution and the transition to homogeneity. *ArXiv e-prints*, October 2018.
- [41] Pierros Ntelis, Anne Ealet, Stephanie Escoffier, et al. The scale of cosmic homogeneity as a standard ruler. *arXiv e-prints*, art. arXiv:1810.09362, October 2018.
- [42] Kyle S Dawson, David J Schlegel, Christopher P Ahn, et al. The baryon oscillation spectroscopic survey of SDSS-III. *The Astronomical Journal*, 145(1):10, 2012.
- [43] S. Alam, M. Ata, S. Bailey, et al. The clustering of galaxies in the completed SDSS-III Baryon Oscillation Spectroscopic Survey: cosmological analysis of the DR12 galaxy sample. *Monthly Notices of the RAS*, 470:2617–2652, September 2017. doi: 10.1093/mnras/stx721.
- [44] Bela Abolfathi, D. S. Aguado, Gabriela Aguilar, et al. The Fourteenth Data Release of the Sloan Digital Sky Survey: First Spectroscopic Data from the Extended Baryon Oscillation Spectroscopic Survey and from the Second Phase of the Apache Point Observatory Galactic Evolution Experiment. *The Astrophysical Journal Supplement Series*, 235:42, Apr 2018. doi: 10.3847/1538-4365/aa9e8a.

- [45] James E Gunn, Walter A Siegmund, Edward J Mannery, et al. The 2.5 m telescope of the sloan digital sky survey. *The Astronomical Journal*, 131(4):2332, 2006.
- [46] Daniel J. Eisenstein, David H. Weinberg, Eric Agol, et al. SDSS-III: Massive Spectroscopic Surveys of the Distant Universe, the Milky Way, and Extra-Solar Planetary Systems. *Astronomical Journal*, 142:72, Sep 2011. doi: 10.1088/0004-6256/142/3/72.
- [47] Shadab Alam, Franco D Albareti, Carlos Allende Prieto, et al. The eleventh and twelfth data releases of the Sloan Digital Sky Survey: final data from SDSS-III. *The Astrophysical Journal Supplement Series*, 219(1):12, 2015.
- [48] Beth Reid, Shirley Ho, Nikhil Padmanabhan, et al. SDSS-III Baryon Oscillation Spectroscopic Survey Data Release 12: galaxy target selection and large-scale structure catalogues. *Monthly Notices of the Royal Astronomical Society*, 455(2):1553–1573, 2016.
- [49] Julian E. Bautista, Mariana Vargas-Magaña, Kyle S. Dawson, et al. The SDSS-IV Extended Baryon Oscillation Spectroscopic Survey: Baryon Acoustic Oscillations at Redshift of 0.72 with the DR14 Luminous Red Galaxy Sample. *Astrophysical Journal*, 863: 110, August 2018. doi: 10.3847/1538-4357/aacea5.
- [50] Pierre Laurent, Sarah Eftekharzadeh, Jean-Marc Le Goff, et al. Clustering of quasars in SDSS-IV eBOSS: study of potential systematics and bias determination. *Journal of Cosmology and Astro-Particle Physics*, 2017:017, July 2017. doi: 10.1088/1475-7516/2017/07/017.
- [51] Pauline Zarrouk, Etienne Burtin, Héctor Gil-Marín, et al. The clustering of the SDSS-IV extended Baryon Oscillation Spectroscopic Survey DR14 quasar sample: measurement of the growth rate of structure from the anisotropic correlation function between redshift 0.8 and 2.2. *Monthly Notices of the RAS*, 477:1639–1663, June 2018. doi: 10.1093/mnras/sty506.
- [52] Will J. Percival, Licia Verde, and John A. Peacock. Fourier analysis of luminosity-dependent galaxy clustering. *Monthly Notices of the RAS*, 347:645–653, Jan 2004. doi: 10.1111/j.1365-2966.2004.07245.x.
- [53] Martin White, Jeremy L Tinker, and Cameron K McBride. Mock galaxy catalogues using the quick particle mesh method. *Monthly Notices of the Royal Astronomical Society*, 437(3):2594–2606, 2014.
- [54] Andy Taylor, Benjamin Joachimi, and Thomas Kitching. Putting the precision in precision cosmology: How accurate should your data covariance matrix be? *Monthly Notices of the RAS*, 432:1928–1946, Jul 2013. doi: 10.1093/mnras/stt270.
- [55] Diego Blas, Julien Lesgourgues, and Thomas Tram. The cosmic linear anisotropy solving system (class). part ii: approximation schemes. *Journal of Cosmology and Astroparticle Physics*, 2011(07):034, 2011.
- [56] Stephen D Landy and Alexander S Szalay. Bias and variance of angular correlation functions. *The Astrophysical Journal*, 412:64–71, 1993.

- [57] J. Rich. Which fundamental constants for cosmic microwave background and baryon-acoustic oscillation? *Astronomy and Astrophysics*, 584:A69, December 2015. doi: 10.1051/0004-6361/201526847.
- [58] Luca Amendola, Stephen Appleby, Anastasios Avgoustidis, et al. Cosmology and fundamental physics with the Euclid satellite. *Living Reviews in Relativity*, 21:2, April 2018. doi: 10.1007/s41114-017-0010-3.
- [59] Francesco Montanari and Ruth Durrer. Measuring the lensing potential with tomographic galaxy number counts. *Journal of Cosmology and Astroparticle Physics*, 2015(10):070, 2015.
- [60] Pierre Laurent, Sarah Eftekharzadeh, Jean-Marc Le Goff, et al. Clustering of quasars in SDSS-IV eBOSS: study of potential systematics and bias determination. *Journal of Cosmology and Astro-Particle Physics*, 2017:017, July 2017. doi: 10.1088/1475-7516/2017/07/017.
- [61] Savvas Nesseris and Manuel Trashorras. Can the homogeneity scale be used as a standard ruler? *arXiv e-prints*, art. arXiv:1901.02400, Jan 2019.
- [62] Kyle S Dawson, Jean-Paul Kneib, Will J Percival, et al. The SDSS-IV extended baryon oscillation spectroscopic survey: overview and early data. *The Astronomical Journal*, 151(2):44, 2016.
- [63] Amir Aghamousa, Jessica Aguilar, Steve Ahlen, et al. The DESI Experiment Part I: Science, Targeting, and Survey Design. *arXiv preprint arXiv:1611.00036*, 2016.
- [64] L. Amendola, S. Appleby, A. Avgoustidis, et al. Cosmology and Fundamental Physics with the Euclid Satellite. *ArXiv e-prints*, jun 2016.
- [65] LSST Science Collaboration, P. A. Abell, J. Allison, et al. LSST Science Book, Version 2.0. *ArXiv e-prints*, dec 2009.
- [66] Peter E Dewdney, Peter J Hall, Richard T Schilizzi, and T Joseph LW Lazio. The square kilometre array. *Proceedings of the IEEE*, 97(8):1482–1496, 2009.
- [67] P. Ntelis. Observational systematics on cosmic homogeneity. In preparation.
- [68] Pierros Ntelis. *Probing Cosmology with the homogeneity scale of the Universe through large scale structure surveys*. Theses, Astroparticule and Cosmology Group, Physics Department, Paris Diderot University, Sep 2017. URL <https://hal.archives-ouvertes.fr/tel-01674537>.